

## A morphological analysis of fresh and brine-cured olives attacked by *Bactrocera oleae* using light microscopy and ESEM-EDS

Barbara Lanza,<sup>1</sup> Anna Panato,<sup>2</sup> Laura Valentini,<sup>3</sup> Pamela Rodegher,<sup>2</sup> Federica Bortolotti,<sup>2</sup> Michela Battistelli,<sup>3</sup> Paolino Ninfali,<sup>3</sup> Pietro Gobbi<sup>3</sup>

<sup>1</sup>*Council for Agricultural Research and Economics (CREA), Research Centre for Engineering and Agro-Food Processing (CREA-IT), Pescara*

<sup>2</sup>*Department of Diagnostics and Public Health, University of Verona*

<sup>3</sup>*Department of Biomolecular Sciences, University of Urbino "Carlo Bo", Urbino (PU), Italy*

### ABSTRACT

The present study investigated the morphology of fresh and brine-cured table olives (TOs) as well as the changes that occur when drupes are attacked by the fruit fly *Bactrocera oleae*. Morphological analyses were performed using light microscopy (LM) and environmental scanning electron microscopy coupled with energy dispersive spectroscopy (ESEM-EDS). The LM analysis was carried out with bright-field microscopy to evaluate sections stained with either PAS or Azan mixtures as well as unstained sections observed at fluorescence microscopy. The results of the analyses showed that: i) Azan and PAS staining played a useful complementary role, increasing the information provided by the histological analysis. Indeed, in both fresh and brine-cured TOs, epidermal layers and mesocarpal cells were clearly revealed, including sclereid cells. The histological analysis allowed also identifying the presence of secoiridoid-biophenols (seco-BPs) in both cell walls and vacuoles, as well as in the drupe regions that had been attacked by fruit flies, where they were found at higher concentrations; ii) In fresh and brine-cured olives, the excitation at 480 nm revealed the distribution of the fluorophores, among which the seco-BP are enclosed; iii) the ESEM-EDS analysis revealed the natural morphology of fresh olives, including the dimensions of their cell layers and the size and depth of the mechanical barriers of suberized or necrotic cells around the larva holes. In addition, the elemental composition of regions of interest of the drupe was determined in fresh and brine-cured TOs. The results highlighted the effectiveness of combined use of LM and ESEM-EDS in order to obtain a picture, as complete as possible, of the structural morphology of TOs. Such analytical combined approach can be used to support multidisciplinary studies aimed at the selection of new cultivars more resistant to fly attack.

**Key words:** Table olives; olive fruit fly; autofluorescence; Azan; PAS reaction; ESEM; EDS.

**Correspondence:** Pietro Gobbi, Department of Biomolecular Sciences (DiSB), Campus Scientifico "Enrico Mattei", University of Urbino "Carlo Bo", Room 707, Via Ca' le Suore 2, Località Crocicchia, 61029 Urbino (PU), Italy. Tel. +39.0722.304244. E-mail: [pietro.gobbi@uniurb.it](mailto:pietro.gobbi@uniurb.it)

**Contributions:** BL, PN, PG, substantial contributions to the conception or design of the work; AP, LV, PR, data acquisition; BL, AP, LV, PR, data analysis; BL, FB, MB, PN, PG, data interpretation; BL, FB, PN, PG, manuscript drafting; BL, FB, MB, PN, PG, manuscript critical revision for important intellectual content.

BL, PN, PG, agree to be accountable for all aspects of the work in ensuring that questions related to the accuracy or integrity of any part of the work are appropriately investigated and resolved. All the authors have read and approved the final version of the manuscript to be published.

**Conflict of interest:** The Authors declare that there is no conflict of interest.

**Funding:** The paper publication was supported by funds of Dottorato Innovativo di ricerca in Biomolecular and health sciences (ciclo XXXV), financed by Regione Marche.

## Introduction

The olive (*Olea europaea* L.) is a drupe whose shape may be elongated, ovoid or spheroidal depending on the cultivar and the growing conditions. A section of the fruit shows three well defined layers: epicarp (or skin), mesocarp (or pulp) and endocarp (or stone). The morphological structure of olive fruit is well described by several authors.<sup>1-3</sup> The epicarp constitutes 1-3% of the fruit; its color varies from green to dark purple, to nearly black, depending on the ripening time and the particular cultivar. It is composed of an external waxy layer consisting of epicuticular waxes, a cuticle of cutin, intracuticular waxes and a monolayer of pyramidal epidermal cells. The cuticle confers rigidity to the tissues, acts as a barrier to biotic and abiotic stresses and increases the impermeability of the epicarp to water. The mesocarp constitutes 65-85% of the fruit and consists of 2-3 layers of elongated cells, close to the layer of epidermal cells, which are composed of the hypodermis and several layers of rounded and gradually more elongated parenchymal cells containing vacuoles with oil droplets and phenols. Most of the oil (8-30 g/100 g of fresh pulp) and compounds which have the organoleptic properties of the fruit accumulate in the mesocarp. The distinguishing elements of the mesocarp are the sclereids, cells with thick lignified cell walls.<sup>4</sup> The number and distribution of these protecting stone cells vary according to the different varieties of olives. Sclereids can occur in very irregular shapes, although they are usually isodiametric or branched. They generally have a mechanical function, bringing rigidity to the tissues.<sup>4,5</sup> Individual stone cells are implicated also in endocarp tissue sclerification.<sup>6</sup> The endocarp constitutes 15-22% of the fruit and is composed of a woody coating (sclerenchyma) which encloses the seed and contains small quantities of oil. A complete description of its morphology has been reported for the first time by Zafrá *et al.*<sup>7</sup>

The cultivated olive tree is widespread in almost all the regions of Italy and is grown from sea level up to about 900 meters above sea level. The presence of the olive tree in Italy dates back over thousand years, thus favoring a high level of biodiversity as highlighted by the 395 different varieties of cultivated olive trees reported in the Italian Register of Olive Cultivation (Reg. EEC 154/75).<sup>8</sup> Only some varieties of *Olea europaea* cultivated in Italy are specifically suitable for being processed as table olives (TOs), depending on the olive's pulp/stone ratio and texture.<sup>9</sup>

Cultivation techniques, such as fertilization, pruning, irrigation, tillage, and the systems for the harvest, transport and storage of the olives destined for processing as TOs are often the same as those adopted for olive groves destined for oil production. Indeed, little consideration is given to the particular concerns associated with TOs such as parasitic attacks, dents and size.<sup>10</sup>

The principal pest affecting *Olea europaea* L. in the Mediterranean Region is an insect (fly) named *Bactrocera oleae* (Rossi) (= *Dacus oleae*) (Diptera: Tephritidae).<sup>11</sup> The monitoring of the olive fruit fly does not take into account that the intervention threshold for TOs should be lower than the threshold for olives grown for producing oil. For Italian olive groves destined for olive oil production, the active infestation threshold is about 10-15%, at which point the trees are treated with larvicides. However, a number of studies, which may lead to a modification of the intervention threshold are currently underway.<sup>12,13</sup> The threshold is considerably lower (max 1%) for TOs, since even non-fertile or feeding stings of the fly can disfigure the drupes and depreciate their worth.<sup>14</sup> Notably, the average annual product loss in the Mediterranean basin due to the fruit fly is 30%, but in some years, the percentage can even reach 100%, representing a significant economic issue.

The percentage of infestation of olives depends on the type of cultivar and the degree of ripening of the drupes, while the size of the fruit is not a significant factor.<sup>15</sup> In addition, the epicarp, and in

particular, the epicuticular and cuticular waxes (principally maslinic acid), seem to play a crucial role in providing protection from pathogens.<sup>15-17</sup> In addition, olives, contain several natural components, such as phytoalexins, which are differently involved in the defense, development and communication of the fruit. Finally, the secoiridoid-biophenols (seco-BPs), in addition to their antioxidant properties, provide a chemical barrier against harmful fungi and a toxic defense alarm against insects.<sup>18</sup>

In light of these particular characteristics of the olive that may play an important protecting role against fly attacks, an assessment of the morphological structure and ultrastructure of the drupe could yield valuable information. Hence, in the present study, using optical and electron microscopy, we investigated the morphology of fresh and brine-cured TOs as well as the changes that occur when drupes are attacked by the fruit fly *Bactrocera oleae*. Specifically, we performed the following analyses: i) light microscopy analysis of olive tissues stained with Azan and periodic acid-Schiff (PAS) methods; ii) fluorescence light microscopy analysis to identify and characterize the seco-BPs in olive tissues; iii) ESEM-EDS analysis to assess the dimensions of cell layers and holes excavated by the larvae in the drupe.

## Materials and Methods

### Olive fruit collection and pre-treatment

The olives (*Olea europaea* L.) were hand-harvested at their mature-green stage of ripening (in mid-October 2019) according to the "Catalogue Field of Olive Varieties" of CREA-IT Città Sant'Angelo (Italy).

The collected drupes were divided into two groups. The fruits of the first group immediately underwent the sample treatment for light and electron microscopy (fresh olives), while the drupes of the second group were first processed as 'treated green olives in brine' (Spanish style) according to the trade standards applying to TOs (brine-cured olives).<sup>19</sup> After debittering and washings, the olives were submerged in a 6% NaCl solution (brine) and left to develop a spontaneous lactic fermentation. After 2 months of storage in this brine, when the pH reached a value of 4.0±0.2, the olives were removed for analysis.

### Bright-field and fluorescence microscopy analysis

The drupes were fixed by immersion in 10% buffered formalin solution (pH 7 ± 0.2). The fresh olives were kept immersed for 65 h, while the brine-treated olives only for 5 min, since they looked already softened, and then easily cuttable, by the 2-months treatment with NaCl solution.

The samples were then cut along the transverse and longitudinal planes and, after the elimination of the stone, dehydrated with alcohol and immersed in liquid paraffin using the Shandon Excelsior TM Processor (Thermo Electron Corporation, Waltham, MA, USA). After the processing cycle, the samples were embedded in paraffin blocks using a Tissue-Tek Tissue Embedding Console System (Diapath, Bergamo, Italy).

The paraffin blocks were cut into 4-µm-thick sections with an RM2255 microtome (Leica Biosystem, Wetzlar, Germany). The sections were collected on slides and kept in an oven at 40°C overnight. The slides were then deparaffinized with xylene, hydrated with alcohol and distilled water. Both the deparaffinization and hydration processes were performed using an Autostainer XL ST5010 (Leica Biosystem).

The sections obtained using the above described procedure were divided into two groups. The slides of the first group under-

went staining with Azan trichrome or periodic acid–Schiff (PAS) counterstained with Carazzi hematoxylin in order to stain the nuclei, following the procedure adopted by Panato *et al.*<sup>20</sup> The slides belonging to the second group did not undergo any staining procedure. The light microscopy analysis was performed using a Leica DM 2500 microscope provided with the ICC50W digital camera (Leica Microsystem GmbH).

In the unstained 4- $\mu\text{m}$ -thick sections, the fluorescent signal was detected, at average excitation wavelength 480 and 530 emission. In this range, there is the maximum of absorbance of olive oil phenols, as seen by Zandomeneghi *et al.*<sup>21</sup>

### ESEM–EDS analysis

The analyses were performed as reported in a previous paper by the same research group.<sup>22</sup> Briefly, immediately prior to the analyses, fresh and brine-cured olive drupes were cut into perpendicular slices (transversal or longitudinal sections) with a sharp stainless steel razor. The slices were deposited onto the aluminum specimen stubs, previously covered with a conductive carbon adhesive disk (TAAB Ltd., Berks, UK), and analyzed using a FEI Quanta 200 FEG environmental scanning electron microscope (FEI, Hillsboro, OR, USA) equipped with an energy dispersive X-ray spectrometer (EDAX Inc., Mahwah, NJ, USA). The analyses were performed using a focalized electron beam in a vacuum electron gun pressure of 5.0 e-6 mbar. The ESEM was used in a low vacuum mode with a specimen chamber pressure set from 0.80 to 0.91 mbar, an accelerating voltage of 15–20 kV, and a magnification ranging between about 50 and 3300x. The images were obtained by means of the secondary and back-scattered electron detector.

The spectrometer unit was equipped with an ECON (Edax carbon oxygen nitrogen) 6 utw X-ray detector and Genesis Analysis software. Each sample was analyzed with a time count of 100 sec and an Amp time of 51, while the probe current was 290  $\mu\text{A}$ . In order to obtain the semiquantitative data, each analysis has been repeated 10 times for similar morphological feature.

## Results

Figure 1 shows the longitudinal sections of the fresh and brine-cured olive tissues stained with Azan or PAS and examined by light microscopy and unstained sections observed at fluorescence microscopy.

The analyses of both the fresh and brine-cured Azan-stained TOs (Figure 1 A,B and 1E, respectively) clearly show the drupe morphology. From the outer to the inner layer it comprises the following components: the epicarp, with the cuticle and a monolayer of pyramidal epidermal cells; the mesocarp, with its layers of elongated cells (hypoderm) and, contiguously, several layers of rounded and gradually elongated parenchymal cells, including some sclereids stained in pale pink. Magenta-stained phenolic vacuoles are found in all of the layers.

On the other hand, due to the violet staining of the PAS-stained fresh and brine-cured TO sections (Figure 1 C,D and 1G, respectively), the epidermal layers, as well as the mesocarp with the sclereids, are more evident than in the Azan stained sections. However, the phenolic vacuoles are not as distinguishable with the PAS staining as they are with the Azan staining because of the low contrast with the violet staining of the cell walls.

The images of the brine-cured TO sections, obtained by exposing the unstained slides to the excitation light of 480 nm (Figure 1 F,H), allow us to clearly distinguish the network of cell walls due to the presence of phenolic compounds and other fluorophores, located in the vacuoles of the epidermal cells, which showed the

highest fluorescence signals.<sup>23</sup>

The images in Figure 2 show the microscopic analysis of the fresh drupe sections attacked by *Bactrocera oleae*. In particular, the Azan and PAS stained sections (Figure 2 A,B) show the tunnels dug by the larva, and the pupal chamber. It is worth mentioning that the staining of the cell layers next to the larva damage appears more intense than that of the other layers. Both Azan and PAS allow staining the pupa, and it is highly likely that the pink section comprises the digestive apparatus.<sup>24</sup> Figure 2 C,D show the transversal drupe section (stained by Azan and PAS, respectively) of the part of the pupal chamber close to the epicarp. The marked pink PAS staining of the cells along the border of the hole may suggest the presence of a higher concentration of secondary metabolites such as callose, in these cells.<sup>25</sup> Figure 2 E,F shows, at a higher magnification, the edge of the pupal chamber in proximity to the

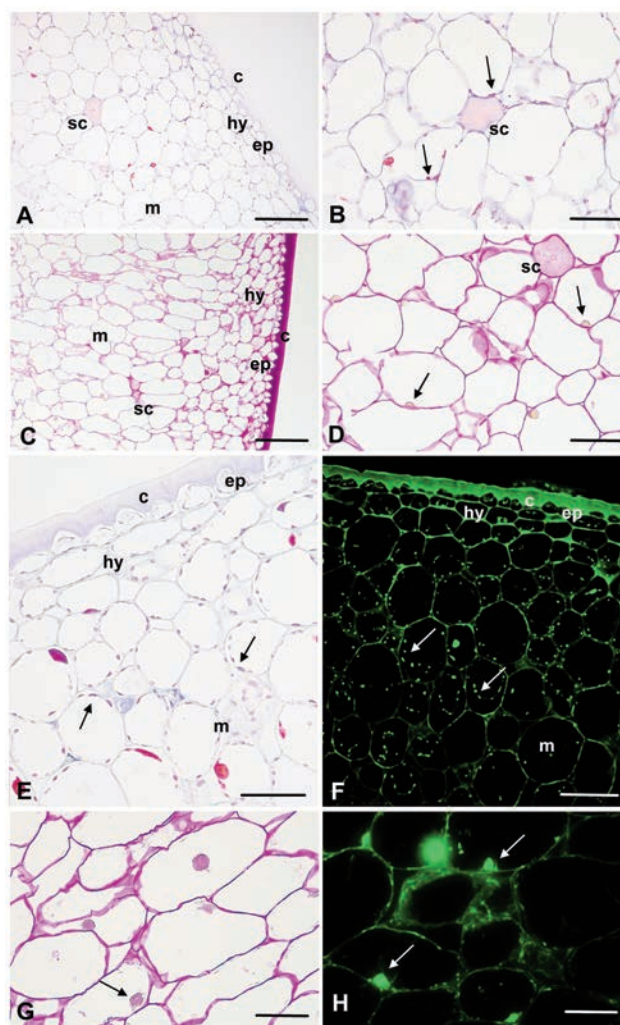


**Figure 1.** Fresh and brine-cured olive tissue sections examined at bright-field and fluorescence microscopy. A,B) Fresh sections stained with Azan trichrome; C,D) fresh sections stained with the periodic acid–Schiff (PAS); E) brine-cured section stained with Azan trichrome; F) unstained brine-cured section observed under fluorescent light; G) brine-cured section stained with the periodic acid–Schiff (PAS); H) unstained brine-cured section observed at fluorescence microscopy. c, cuticle; ep, epidermal cells; hy, hypoderm; m, mesocarp; sc, sclereid; arrow, accumulation of biophenols. Scale bars: A,C) 100  $\mu\text{m}$ ; B,D,E–H) 50  $\mu\text{m}$ .



hole in the cuticle. The increase in the staining intensity still suggests an activation of the production of secondary metabolites, which also involves the sclereid cells. Analysis at fluorescence microscopy (Figure 2 G,H) confirmed the higher phenolic concentration in the cells bordering the pupal chamber as well as in the cell walls of the sclereids.

Figure 3 shows the ESEM analysis of sections of drupes attacked by *Bactrocera oleae*. The tunnels dug by the larva and the pupal chamber are shown in Figure 3 A and B, respectively. The pupal chamber locates at the bottom of the tunnel, which stretches from the middle of the mesocarp towards the hypodermal layer (Figure 3B). The diameter of the bulge measures  $1.56 \pm 0.23$  mm, corresponding to the diameter of the pupal chamber. Figure 3C shows the exit hole of the pupa observed from the outside of the epicarp. Figure 3D shows the area around the tunnels, highlighting the dramatic morphological changes in the cells bordering the hole. The oil drops are only maintained in a few cells, while most of the other cells are empty and compressed. At higher magnifications (Figure 3 E,F), it is possible to observe the morphological changes

**Table 1.** Elemental composition examined by the ESEM-EDS in the same samples as Figure 4A (fresh olives) and 4C (in-brine olives). Wt% = weight percent concentration. The data are expressed as mean of 10 measurements and the coefficient of variation was <5%.

Element	Wt%	
	Fresh	Brine-cured
C	78.05	61.36
N	0.50	3.39
O	18.12	25.34
Na	0.72	5.46
Mg	0.19	0.13
P	0.55	0.17
S	0	0.20
Cl	0.41	3.09
K	0	0.18
Ca	1.46	0.68

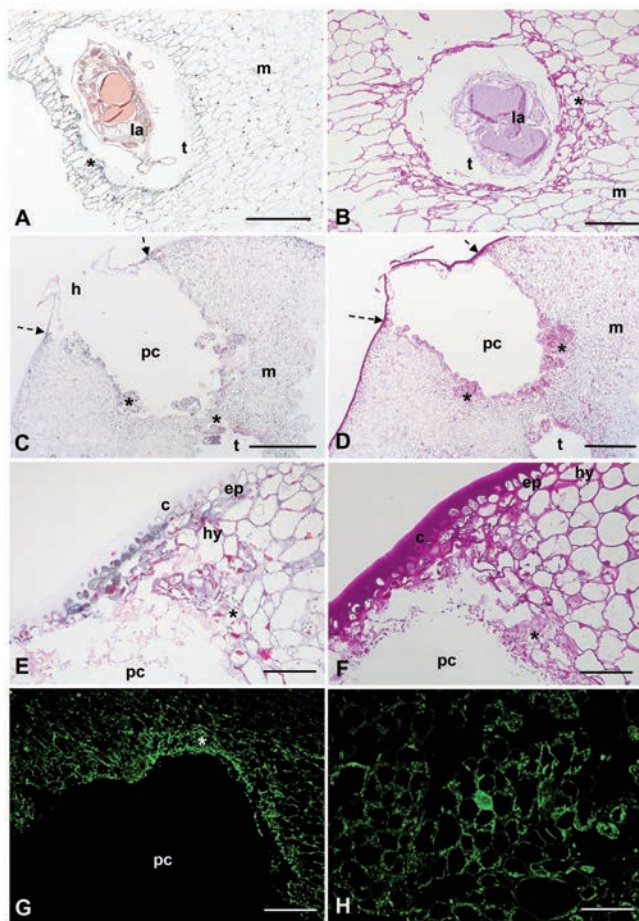


**Figure 2.** Fresh olive fruit tissue sections attacked by *Bactrocera oleae* examined at bright-field and fluorescence microscopy. A,C) Sections stained with Azan trichrome; B,D) sections stained with the periodic acid-Schiff (PAS); E,F) details of suberized area near epidermis; G) unstained sections of the hole zone observed at fluorescence microscopy; H) details of the area with suberized cells. c, cuticle; ep, epidermal cells; hy, hypodermis; m, mesocarp; la, larva; h, exit hole; t, tunnel dug by larva; pc, pupal chamber; arrow, limit of bulge area; \*, suberized cells. Scale bars: A) 500  $\mu$ m; B,G) 200  $\mu$ m; C,D) 1 mm; E,F,H) 100  $\mu$ m.

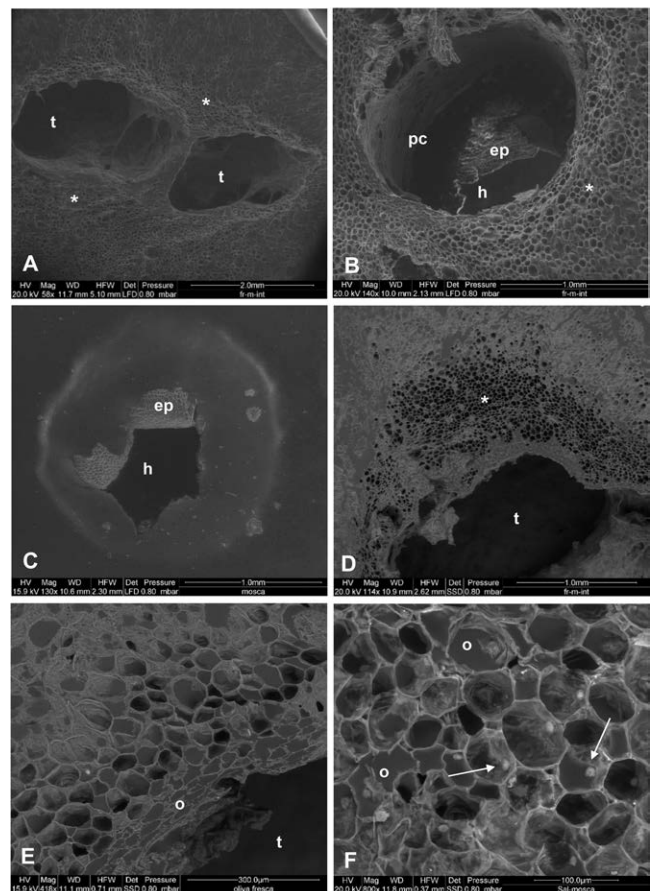


**Figure 3.** Fresh olive fruit tissues attacked by *Bactrocera oleae* examined by ESEM. A) Tunnels dug by the larvae; B) area around the hole seen from the inside; C) area around the hole seen from the outside; D) area around the tunnel; E,F) details of area around the tunnel rich in oil and biophenols. t, tunnel dug by larva; ep, epidermal cells; h, exit hole; pc, pupal chamber; o, oil droplet; \*, suberized cells; arrow, accumulation of biophenols.

that occur on the area surrounding the parasite wound with a curtain of suberized and necrotic cells.<sup>25</sup> Inside the cells that contain no oil, a droplet similar to the accumulation of biophenols described in Figure 1 is also detectable.

Figure 4 shows the ESEM-EDS analysis of the drupe together with its elemental composition. Figure 4A shows cells from a fresh olive with details of the oil droplets. The elemental pattern shown in Figure 4B was obtained by analyzing the squared area highlighted in Figure 4A and looks compatible with the presence of triglycerides, vegetal origin and low concentration of salts. Figure 4C shows cells of the cell walls of a brine-cured olive, with salt formations on the epidermal layer. The pattern shown in Figure 4D reveals the elemental composition of the squared area reported in Figure 4C. As expected, there is a significant presence of the cations Na, Mg, K and Ca in these brine-cured olive cells. The presence of parasite within the sample does not affect the EDS elemental composition (*data not shown*).

Finally, Table 1 shows the concentrations of all the elements detected in the EDS analysis as weight percent values of the elements. Overall, the semiquantitative data confirm the elemental composition of a vegetal sample as well as the elemental addition due to the brining process. Being the elemental analysis semiquantitative with a cut-off at 100%, the addition of Na and Cl in brine-cured samples produces a relatively small imbalance of the other elements compared to the fresh samples.

## Discussion

In this work, LM and ESEM-EDS analyses were used to obtain as much information as possible on the morphology of both fresh and brine-cured TOs in an intact state and after being attacked by flies. The olive sections for LM analysis were treated with the alcohol series, thus leaving the tissue architecture deprived of water and oil. The ESEM-EDS analysis was performed on fresh olive samples, without any chemical treatments, thus allowing us to observe the tissue morphology as well as to draw the elemental composition directly on the food matrix.

Sections for the LM analysis were stained with both the Azan and PAS methods.<sup>20</sup> The Azan and PAS staining provided complementary information on the drupe structure. In particular, the Azan staining highlights the phenolic vacuoles in magenta, thus creating a marked contrast with the blue cell walls. On the other hand, the PAS staining highlights the epicuticular layers and cell walls in a showy pink. Unstained sections, observed at fluorescence microscopy,<sup>21</sup> revealed that most of the fluorophores detected at 530-nm emission following 480-nm excitation, including seco-BP, remained firmly bound to the cells' walls. Observations based on a qualitative analysis suggest that the brine-cured olives have a lower content of fluorophores, and very likely of seco-BP, than fresh olives. Only a specific investigation would allow drawing reliable quantitative data, as the assessment of the fluorescent intensity needs to know which specific fluorophores are present and calibration curves with standard molecules are to be made.<sup>23</sup>

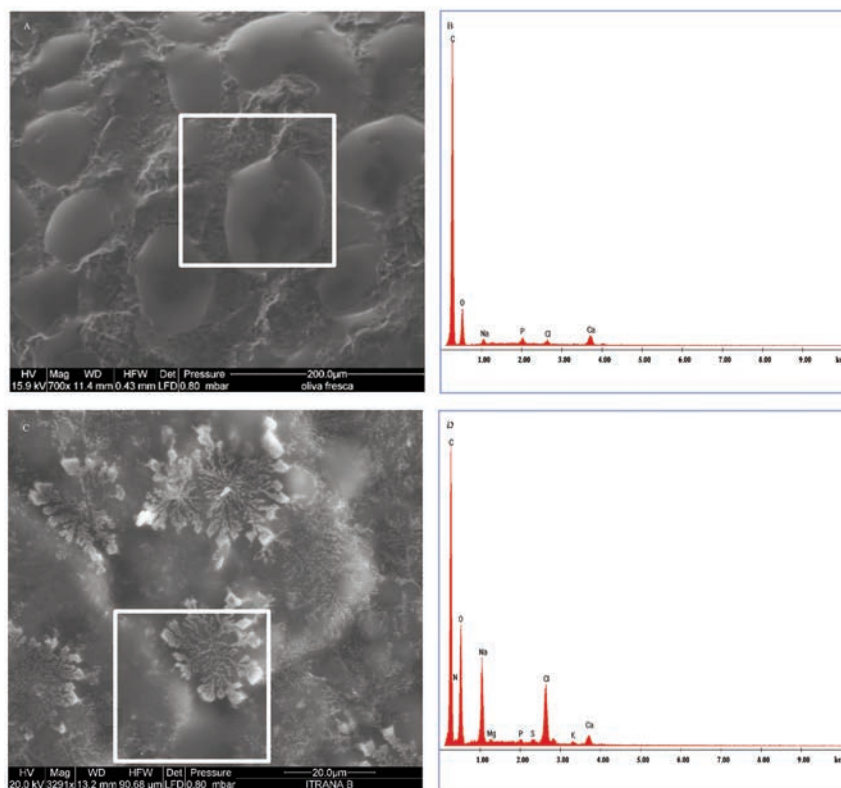


**Figure 4.** Fresh and brine-cured olive tissues examined by ESEM and respective EDS spectra. A) Fresh olive mesocarp cells with oil droplets; C) external epicarp cells of brine-cured olives with NaCl crystals. B and D, respective EDS spectra. The graphs are representative of a single analyzed area.



It is noteworthy that despite the subjectively observed lower fluorescence in the brine-cured olives, the content of phenols is still remarkable and it is reasonable to suppose that their health protecting effect remained significant in the fruit.<sup>9,27</sup> Sections of olives that had been attacked by flies were analyzed in both fresh and brine-cured olive sections in order to evaluate the size and area of the tunnels, holes and pupa. The regions of olive tissues around the hole, stained by both PAS and Azan, revealed that phenol compounds, mostly the seco-BPs, are concentrated in the regions of the parasite attack. Seco-BPs belong to the coordinated gene system of defense that is triggered in the event of pest attacks, together with structural changes to circumscribe the damaged area.<sup>28</sup> Specifically, seco-BPs play an important role in internal communication since increases in their concentration are directly linked to tissue repair mechanisms.<sup>29</sup> The active metabolism and production of secondary metabolites in these regions were confirmed by the analysis at fluorescence microscopy, which showed an increase in intensity.

The developmental stages and characteristics of the niche where the larvae and pupae evolve were thoroughly investigated by ESEM-EDS analysis. The larva galleries and their irregular and tortuous tunnels increase in size as the larvae grow. Sometimes the tunnels have bifurcations with a secondary branch, which is generally a dead end. The ESEM analysis provided the exact measurements of the hole diameters and areas,<sup>22</sup> as well the presence of layers of cells with suberized walls around the tunnel walls. It is highly likely that the insect attack causes an increase in the suberization of the walls since suberin deposition protects the olive fruit tissues from more extensive damage and contributes to the creation of an impermeable chemical-physical barrier that limits the attack.<sup>26</sup>

EDS allowed evaluating the elemental concentration in the part of the cells containing deposits of primary and secondary metabolites as well as residual compounds used in processing.<sup>22</sup> For instance, the oil droplets inside the cells showed fat components containing only traces of minerals. On the contrary, the brine-cured olives showed a very high concentration of ions, *i.e.* Ca, K, S, P and Mg, in addition to Na and Cl. No variations have been detected in EDS elemental composition by comparing sound as parasitized samples.

The insights and data provided by these combined microscopy techniques may be useful in the control of fresh and brine-cured olives in terms of their nutritional and morphological characteristics. This work promotes a multidisciplinary approach to develop practical solutions to control the TO food line and to face serious emerging olive diseases. Differences in the tolerance of olive cultivars to fly attacks are related to chemical factors and morphological changes that yield mechanical barriers. Therefore, the selection of more resistant and tolerant cultivars may be guided also by the morphological analysis of the epidermal layer dimensions and resistance. Seco-BPs play a role in structuring the cell wall skeleton<sup>18</sup> and their concentration is very important in the defense against fruit flies. Hence, the ability to describe the progressive morphological changes that occur during the parasite attack by combining measurements of seco-BPs using fluorescence microscopy and measurements of the suberized layers by ESEM could provide insights into the linkage between morphology and gene activation phases.<sup>27</sup> In this kind of approach, microscopy and molecular biology investigations may be complementary tools.<sup>30</sup> The EDS elemental composition of the brine-cured TOs, combined with the fluorescence analysis of the phenolic pool, allows us to control TO salt treatments and washing times in order to adapt the transformation processes to each specific olive cultivar. Hence, we can minimize losses of seco-BPs in the processing and avoid the use of excessive quantities of salt.

## Acknowledgements

The authors wish to thank the ARPAM, Pesaro Department (Pesaro, PU, Italy) for its collaboration with the University of Urbino "Carlo Bo" in the management of the ESEM-EDS Laboratory. We are also grateful to Dr. Andrea Guidarelli of the Department of Biomolecular Sciences at the University of Urbino "Carlo Bo" for his skilled technical assistance at the Fluorescence Microscopy Lab and we are also grateful to Dr. Sara Salucci for critical support in data evaluation.

## References

- Hammami SBM, Rapoport HF. Quantitative analysis of cell Organization in the external region of the olive fruit. *Int J Plant Sci* 2012;173:993-1004.
- Bianchi G. Lipids and phenols in table olives. *Eur J Lipid Sci Technol* 2003;105:229-42.
- Grande MD, Tamayo AI. Estudios sobre la estructura histologica del fruto de *Olea europaea* L. I. Variedad Zorzalena. *Grasas y Aceites* 1964;15:72-80.
- Marsilio V, Lanza B, De Angelis M. Olive cell wall components: physical and biochemical changes during processing. *J Sci Food Agric* 1996;70:35-43.
- Dekazos ED. Sclereid development and prevention of woodiness and/or grittiness in rabbiteye blueberries. *Proc Florida State Hortic Soc* 1977;90:218-24.
- Hammami SBM, Costagli G, Rapoport HF. Cell and tissue dynamics of olive endocarp sclerification vary according to water availability. *Physiol Plantarum* 2013;149:571-82.
- Zafra A, M'rani-Alaoui M, Lima E, Jimenez-Lopez JC, Alché JD. Histological features of the olive seed and presence of 7S-type seed storage proteins as hallmarks of the olive fruit development. *Front Plant Sci* 2018;9:1481.
- European Commission. Regulation (EEC) No 154/75 of the Council of 21 January 1975 on the establishment of a register of olive cultivation in the Member States producing olive oil. *OJ L* 19, 24.1.1975.
- Lanza B. Nutritional and sensory quality of table olives. In: Muzzalupo I, editor. *Olive germplasm - The olive cultivation, table olive and olive oil industry in Italy*. Rijeka; InTech: 2012.
- Garrido Fernández A, Fernández Díez MJ, Adams MR. *Table olives. Production and processing*. London, Chapman & Hall; 1997.
- Tzanakakis ME. Olive Fruit Fly, *Bactrocera oleae* (Rossi) (= *Dacus oleae*) (Diptera: Tephritidae). In: Capinera JL, editor. *Encyclopedia of entomology*. Dordrecht: Springer; 2008.
- Caleca V, Antista G, Campisi G, Caruso T, Lo Verde G, Maltese M, et al. High quality extra virgin olive oil from olives attacked by the olive fruit fly, *Bactrocera oleae* (Rossi) (Diptera Tephritidae): which is the tolerable limit? data from experimental 'Nocellara del Belice' and 'Cerasuola' olive groves in Sicily. *Chem Eng Trans* 2017;58:451-6.
- Gucci R, Caruso G, Canale A, Loni A, Raspi A, Urbani S, et al. Qualitative changes of olive oils obtained from fruits damaged by *Bactrocera oleae* (Rossi). *HortScience* 2012;47:301-6.
- Caleca V, Rizzo R. Soglie di dannosità e controllo di *Bactrocera oleae* (Rossi) nell'olivicultura biologica da tavola. In: *Agricoltura Biologica: sistemi produttivi e modelli di commercializzazione e di consumo*. IV Workshop GRAB-IT, 2009;359-62.
- Kombargi WS, Michelakis SE, Petrakis CA. Effect of olive

- surface waxes on oviposition by *Bactrocera oleae* (Diptera:Tephritidae). *J Econ Entomol* 1998;91:993-8.
16. Lanza B, Di Serio MG. SEM characterization of olive (*Olea europaea* L.) fruit epicuticular waxes and epicarp. *Sci Hortic* 2015;191:49-56.
  17. Rebora M, Salerno G, Piersanti S, Gorb E, Gorb S. Role of fruit epicuticular waxes in preventing *Bactrocera oleae* (Diptera:Tephritidae) attachment in different cultivars of *Olea europaea*. *Insects* 2020;11:189.
  18. Uccella N. Olive biophenols: biomolecular characterization, distribution and phytoalexin histochemical localization in the drupes. *Trends Food Sci Technol* 2001;11:315-27.
  19. International Olive Council. Trade standards applying to table olives. Document COI/OT/NC No. 1. Madrid: International Olive Council; 2004. Available from: <http://www.internationaloliveoil.org/estaticos/view/224-testing-methods>
  20. Panato A, Antonini E, Bortolotti F, Ninfali P. The histology of grain caryopses for nutrient location: a comparative study of six cereals. *Int J Food Sci Tech* 2017;52:1238-45.
  21. Zandomenighi M, Carbonaro L, Caffarata C. Fluorescence of vegetable oils: olive oils. *J Agric Food Chem* 2005;53:759-66.
  22. Antonini E, Zara C, Valentini L, Gobbi P, Ninfali P, Menotta M. Novel insights into pericarp, protein body globoids of aleurone layer, starchy granules of three cereals gained using atomic force microscopy and environmental scanning electronic microscopy. *Eur J Histochem* 2018;62:2869.
  23. Sikorska E, Khmelinskii I, Sikorski M. Analysis of olive oils by fluorescence spectroscopy: methods and applications. In: Boskou D, editor. *Olive oil - constituents, quality, health properties and bioconversions*. Rijeka: InTech; 2012.
  24. Martin-Vega D, Simonsen TJ, Hall MJR. Looking into the puparium: Micro-CT visualization of the internal morphological changes during metamorphosis of the blow fly, *Calliphora vicina*, with the first quantitative analysis of organ development in Cyclorrhaphous dipterans. *J Morphol* 2017;278:629-51.
  25. Nowicki M, Lichočka M, Nowakowska M, Klosinska U, Golik P, Kozik EU. A simple dual stain for detailed investigations of plant-fungal pathogen interactions. *Veg Crop Res Bull* 2012;77:61-74.
  26. Kombrink E, Somssich IE. Defence responses of plants to pathogens. *Adv Bot Res* 1995;21:1-34.
  27. Lanza B, Ninfali P. Antioxidants in extra virgin olive oil and table olives: connections between agriculture and processing for health choices. *Antioxidants* 2020;9:41.
  28. Corrado G, Garonna A, Gómez-Lama Cabanás C, Gregoriou M, Martelli GP, Mathiopoulou KD, et al. Host response to biotic stresses. In: Rugini E, Baldoni L, Muleo R, Sebastiani L, editors, *The olive tree genome*. Cham, Switzerland: Springer International Publishing; 2016.
  29. Servili M, Sordini B, Esposto S, Taticchi A, Urbani S, Sebastiani L. Metabolomics of olive fruit: a focus on the secondary metabolites. In: Rugini E, Baldoni L, Muleo R, Sebastiani L, editors. *The olive tree genome*. Cham: Springer; 2016.
  30. Ninfali P, Panato A, Bortolotti F, Valentini L, Gobbi P. Morphological analysis of the seeds of three pseudocereals by using light microscopy and ESEM-EDS. *Eur J Histochem* 2020;64:3075.

---

Received for publication: 8 June 2020. Accepted for publication: 2 September 2020.

This work is licensed under a Creative Commons Attribution-NonCommercial 4.0 International License (CC BY-NC 4.0).

©Copyright: the Author(s), 2020

Licensee PAGEPress, Italy

*European Journal of Histochemistry* 2020; 64:3149

doi:10.4081/ejh.2020.3149